https://doi.org/10.3311/PPci.37882
Creative Commons Attribution

Periodica Polytechnica Civil Engineering

Investigating the Site Response Variability of Deep Sedimentary Column Induced by Varying Soil Friction Angles

Amit Prajapati[1*], Bin Zhao[1]

[1] State Key Laboratory of Disaster Reduction in Civil Engineering, Tongji University, 1239 Siping Road, 200092 Shanghai, China
[*] Corresponding author, e-mail: binzh@tongji.edu.cn

Received: 23 July 2024, Accepted: 31 October 2024, Published online: 22 November 2024

Abstract

Ensuring the danger level for sustainable development requires a proper ground response analysis with reliable geological properties of deep sediment deposits up to bedrock. The seismic assessment procedure commonly dealth with the upper 30 meters of soil, overlooking the influence of deeper sediment layers. This study performs the seismic response of an entire soil column extending to bedrock, accounting for the soil frictional angle variability. A one-dimensional nonlinear ground response analysis was conducted using 28 earthquake records, with soil friction angles ranging from 10 to 60 degrees. The results highlight the nonlinear behavior of soils, particularly the modification of shear modulus and damping ratio with depth, influenced by changes in frictional angle and effective vertical stress. It indicates that the 10° frictional angles produce a minimum spectral acceleration demand, primarily due to the high energy dissipation in the over-softened upper layer, hence, reduction in peak ground acceleration (PGA). While a 30° friction angle produces high spectral acceleration at short period in shallow depth. The seismic response resulted in a 0.54 times decrease in peak acceleration in the ground relative to bedrock, highlighting the significance of deep soil investigation. This study shows that different friction angles present a greater understanding of seismic site response, leading to better hazard assessment insights.

Keywords

nonlinear analysis, deep sediment, frictional angle, peak ground acceleration, acceleration response spectra

1 Introduction

Investigating site response analysis in deep sediment deposits is essential to comprehending the substantial impacts on the seismic behavior of residential buildings and the long-term viability of growing infrastructure. Urban cities like Mexico City (Mexico) and Kathmandu Valley (Nepal), located in deep basins, have experienced numerous significant earthquakes, illustrating the need for accurate prediction of seismic hazards [1]. Seismic assessment in such cities can be better understood by considering overall soil depth, which accounts for the variability in lacustrine deposits across time. The seismic response prediction for general structures, except for complex subsurface geology, very much suitable considering only the shear wave velocity of the first 30 m of depth (Vs30). Vs30 is a widely used parameter for classifying site conditions and seismic assessment presented in building codes, such as Eurocode 8 [2]. However, it fails to account for seismic prediction of deep soil layers beyond 30 m with different impedance ratio [3, 4]. It is likely to predict unreliable response spectra for the sedimentary basin by emphasizing the Vs30, which does not account for the whole frequency range. Eurocode 8 suggested performing deep soil analysis where long-period seismic waves are dominant, especially in sedimentary basins or complex subsurface structures. The significance of considering deep sediments when analyzing the nonlinear ground response of soils is highlighted by thorough literature studies, like the one provided by Zahoor et al. [4]. In addition, soil's inherent properties significantly affect the prediction of nonlinear seismic ground responses, including soil stress, damping frictional angle, and dynamic soil characteristics.

Moreover, soil discreteness plays a crucial in shaping its nonlinear dynamic behavior. The degree of discreteness directly impacts nonlinearity, which influences strain amplitude during seismic events. Also, the shear modulus tends to drop with increasing discreteness while the damping ratio increases, augmenting the soil's nonlinear responses [5]. Notably, the shear modulus reduction is less

Cite this article as: Prajapati, A., Zhao, B. "Investigating the Site Response Variability of Deep Sedimentary Column Induced by Varying Soil Friction Angles", Periodica Polytechnica Civil Engineering, 2024. https://doi.org/10.3311/PPci.37882

pronounced at a high effective stress [6]. The resistance of each soil layer is primarily influenced by the effective stress and the interaction between soil grains, which can be represented by friction angle. However, determining the precise frictional angle of soil at a different depth presents significant challenges. Consequently, employing a range of frictional angles in ground response analysis is essential for obtaining more accurate and feasible results. Unlike many other factors that influence the soil's dynamic properties, soil frictional angle is a notable trait that alters the soil's stress-strain hardening during seismic activity.

Generally, one-dimensional (1D) ground response analysis predicts the seismic behavior of the ground by modeling vertically propagating shear wave velocity from the underlying bedrock [7]. Depending on the complexity of the site, site response analysis is conducted using linear, equivalent linear (EL), and nonlinear (NL) approaches. The linear approach assumes constant dynamic properties across soil layers, neglecting changes in soil behavior under seismic loading. In contrast, the EL technique provides better accuracy than the linear model under moderate seismic responses by approximating nonlinear soil behavior, combining linear soil parameters with adjustments for nonlinear seismic response [8]. However, the NL approach provides a more robust solution by accounting for the full nonlinear response of soil through incremental analysis [9]. Linear approximations fail to accurately capture ground motions when shear strains are large, particularly in soft or loose soils, demanding a completely nonlinear site response analysis to estimate surface motion accurately. Generally, the EL approach provides reliable results in shallow soil, excluding very soft soils, for peak ground acceleration (PGA) in the range of 0.1 to 0.2 g [10]. Meanwhile, the nonlinear approach predicts a better response when the strain value exceeds 0.05% [9].

Further, the soil's shear strain index significantly influences EL and NL ground response analysis approaches [11]. Likewise, inaccurate prediction of soil shear strength leads to erroneous interpretation of surface responses [12]. Furthermore, nonlinear ground response analysis is essential for accurately capturing the soil's nonlinear behavior as seismic waves propagate from bedrock to the surface, as Hashash et al. [13] highlighted in the computer-based program DEEPSOIL. This approach accounts for strain-dependent changes in soil stiffness, providing a more precise assessment of ground motion during seismic events.

Numerous researchers adopted DEEPSOIL [13] to simulate the soil deposit under seismic excitation for performing a 1D nonlinear site response analysis [11, 14–16]. This computer program incorporates the theoretical framework and computational procedure for simulating 1D linear, equivalent linear, and nonlinear site response analysis. While two-dimensional and three-dimensional analyses account for comprehensive nonlinear site response analysis, their response's effectiveness depends on the appropriate use of complex boundary conditions and Rayleigh damping [17]. Bard and Gariel [18] presented a strong agreement between the one and two-dimension amplification at the center and edges of the deep valley. Similarly, the reliability of 1D nonlinear site response analysis performed in DEEPSOIL was validated with established sites of Kiban-Kyoshin (KiK-net) vertical array station in Japan by researchers [9, 16]. Bolisetti et al. [14] studied the seismic analysis of nuclear structures from different approaches using various available programs, including DEEPSOIL, and found that the associated acceleration response is unaffected despite the notable differences in the peak strain across consecutive layers. Nguyen et al. [19] performed a 1D site response analysis to evaluate the applicability of the Vietnamese earthquake resistance design code.

This study predicts the ground response of 28 earthquakes by performing 1D site response at the deep soil deposits by altering the wide range of frictional angles. The analysis in the nonlinear program DEEPSOIL evaluates the ground responses at different depths while accounting for variations in soil's dynamic properties and effective vertical stress. This study highlights the spectral acceleration response generated at different depths by employing a range of frictional angles from 10 to 60 degrees. Furthermore, it establishes a correlation between the PGA and frictional angle, generating a best-fitting curve based on the input ground motions.

2 Input data

According to the ASCE/SEI 41-06 [20] and NIST [1] guidelines, at least three time histories should be employed while performing nonlinear dynamic analysis of the structures. For critical or significant structures, the number of time histories is increased to enhance the reliability of the analysis. It is recommended that an average response of at least seven times the historical response should be used to accurately assess existing structures. In this study, a total of 28 ground motions (GMs) were selected from the PEER Ground Motion Database [21] to satisfy these requirements and ensure a comprehensive analysis of the existing significant structures. All the ground motions were best fitted to the implied parameters and the target response spectrum employed on the web-based system. The uniform

Hazard Spectrum prepared by [22], with a return period of 475 years and a PGA of 0.424 g, is used as the target spectrum in the study. A suite of horizontal ground motion components spectrum is constructed by taking a square root of the sum of the squares of the five percentage damped response spectra. The time histories and target spectrum are matched with the quantitative measures using mean square error. In this study, ground motion with shear velocity (Vs30) greater than 700 m/s was considered bedrock conditions. Similarly, other selection parameters include earthquake events with a magnitude greater than 5 Mw, rupture distance (*Rrup*), the time interval at which 5% and 95% of Arias intensity (D5-95) and Joyner-Boore distance (*Rjb*) less than 100 Km. The selected ground motions for the study are listed in Table 1.

The selected ground motions were adjusted to make them compatible with the target spectrum using the spectral matching technique. The matching was performed in SEISMOMATCH, which alters the time series data frequency according to the target spectrum. This method preserves the nonstationary characteristic of ground motions even after modification of amplitude and time [23]. The maximum period for spectral matching is restricted to 4.0 s and iteration to 30 times due to inconsistent nonstationary characteristics when using a higher period. The adjusted 4 s matching was performed in two steps for the reliability of GMs and convergence criteria. In the first step, the spectra matching up to 1.0 s were performed to properly adjust the peak of spectral matching to ignore the influences of long periods. After that, only those time series motions that pass the convergent criteria were processed to the second step, where 4 s spectral matching was done. All the converged time series from the spectral matching were the input for the nonlinear ground response analysis.

Table 1 Ground motion selected for the nonlinear ground response analysis

ID	RSI	Earthquake name	Year	Mw	Mechanism	*Rjb* (km)	*Rrup* (km)	Vs30 (m/s)	PGA (g)
1	43	Lytle Creek	1970	5.33	Reverse Oblique	17.4	19.35	813.48	0.09
2	80	San Fernando	1971	6.61	Reverse	21.5	21.5	969.07	0.08
3	98	Hollister-03	1974	5.14	Strike-slip	9.99	10.46	1428.14	0.09
4	143	Tabas_ Iran	1978	7.35	Reverse	1.79	2.05	766.77	0.64
5	225	Anza Horse Canyon	1980	5.19	Strike-slip	12.24	17.26	724.89	0.04
6	454	Morgan Hill	1984	6.19	Strike-slip	14.83	14.84	729.65	0.11
7	4312	Umbria-03_ Italy	1984	5.6	Normal	14.67	15.72	922	0.03
8	3718	Whittier Narrows-02	1987	5.27	Reverse Oblique	25.04	28.42	1222.52	0.01
9	763	Loma Prieta	1989	6.93	Reverse Oblique	9.19	9.96	729.65	0.19
10	809	Loma Prieta	1989	6.93	Reverse Oblique	12.15	18.51	713.59	0.22
11	1649	Sierra Madre	1991	5.61	Reverse	37.63	39.81	996.43	0.03
12	879	Landers	1992	7.28	Strike-slip	2.19	2.19	1369	0.82
13	1011	Northridge-01	1994	6.69	Reverse	15.11	20.29	1222.52	0.10
14	1012	Northridge-01	1994	6.69	Reverse	9.87	19.07	706.22	0.18
15	1091	Northridge-01	1994	6.69	Reverse	23.1	23.64	996.43	0.09
16	1108	Kobe_ Japan	1995	6.9	Strike-slip	0.9	0.92	1043	0.45
17	1161	Kocaeli_ Turkey	1999	7.51	Strike-slip	7.57	10.92	792	0.19
18	1165	Kocaeli_ Turkey	1999	7.51	Strike-slip	3.62	7.21	811	0.14
19	1257	Chi-Chi_ Taiwan	1999	7.62	Reverse Oblique	52.46	56.14	1525.85	0.05
20	1485	Chi-Chi_ Taiwan	1999	7.62	Reverse Oblique	26	26	704.64	0.35
21	8165	Duzce_ Turkey	1999	7.14	Strike-slip	4.21	4.21	760	0.33
22	2019	Gilroy	2002	5.0	Strike-slip	2.21	8.27	729.65	0.08
23	4438	Molise-02_ Italy	2002	5.7	Strike-slip	49.6	51.32	865	0.09
24	4083	Parkfield-02_ CA	2004	6.0	Strike-slip	4.66	5.29	906.96	0.07
25	4167	Niigata_ Japan	2004	6.63	Reverse	52.15	52.3	828.95	0.08
26	5618	Iwate_ Japan	2008	6.9	Reverse	16.26	16.27	825.83	0.20
27	4483	L'Aquila_ Italy	2009	6.3	Normal	0	5.38	717	0.37
28	1613	Duzce, Turkey	1999	7.14	Strike-slip	25.78	25.88	782	0.002

3 Evaluation of ground response analysis

Sand and gravelly sand are classified as cohesionless materials, with fine particles influencing the level of discreteness within the soil matrix. In highly discrete materials devoid of fine particles, contacts between soil layers are established without significant frictional bonding. The discreteness influences the dynamic nonlinear properties of each soil layer, characterized by shear modulus and damping ratio. Since the expected soil parameters from the laboratory or field experiments are not always achievable for all locations, a range of dynamic properties is employed to construct the hyperbolic model for analysis.

This study examines a 269 m depth soil column [24] from the deep sediment site of Kathmandu Valley (Nepal), along with its shear velocity model, as shown in Fig. 1 (a) and (b). It focuses on the influences of soil discreteness in 1D nonlinear analysis by altering the friction angle from 10 to 60 degrees for deep sediment. Table 2 shows the relationship between the frictional angle and (τ_{max}/σ_v') calculated from Eq. (1), where τ_{max} is the maximum shear strength and σ_v' is the effective vertical stress. Frictional angles below 30° are considered loose soil, while above 30° are dense soil. The friction angle beyond 60 degrees behaves like solid or rigid bodies, which are unavailable in nature. As the friction angle changes, the variation in the nonlinear properties of each layer, such as shear modulus and damping ratio, are evaluated with the shear strain as presented in the systematic diagram in Fig. 1 (d). The maximum shear strength of the soil model [25] was calculated using different frictional angle in soil layers using the Eq. (1):

$$\left.\begin{aligned} K_0 &= \left(1-\sin\left(\varnothing\right)\right)\times \mathrm{OCR}^{\sin(\varnothing)} \\ \sigma_m' &= \sigma_v'\left(1+2K_0\right)/3 \\ \tau_{\max} &= \sigma_m' \sin\left(\varnothing\right) \end{aligned}\right\} \quad (1)$$

K_0 = effective earth pressure,
$\varnothing$ = frictional angle of soil,
OCR = over consolidation ratio,
σ_m' = mean effective vertical pressure,
$\tau_{\max}$ = maximum shear strength.

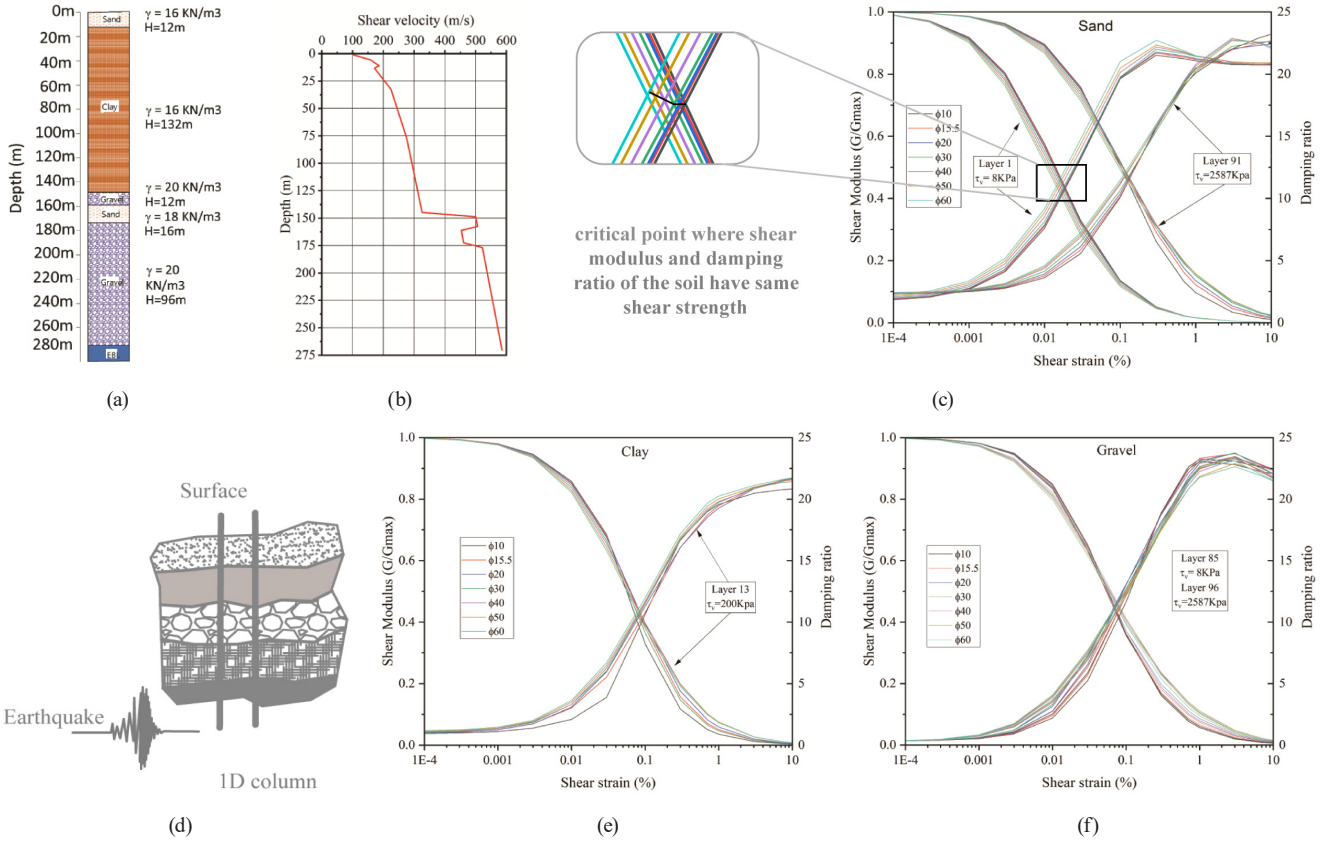

Fig. 1 Dynamic characteristic of the soil (a) the deep soil column showing individual layers and its basic properties, (b) shear wave velocity along with the depth, (c) dynamic characteristic of the sand at Layer 1 and Layer 91, (d) general representation of 1D ground soil column (e) dynamic characteristic of clay at Layer 13, and (f) dynamic characteristic of gravel at Layers 85 and 96

Table 2 Effective stress to shear strength (τ_{max}/σ_v') due to change in the frictional angle of soil and the discreteness of the soil

Frictional angle	10	15	20	30	40	50	60
(τ_{max}/σ_v')	0.153	0.22	0.264	0.333	0.368	0.372	0.363
	Loose soil				Dense soil		

The dynamic response of the ground is initially influenced by shear modulus and damping; however, the actual behavior of the soil under cyclic loading is far more complex than those of these two parameters. The nonlinearity of the soil is represented by the stress-strain behavior of the soil, which exhibits an increase in damping ratio and a reduction of shear modulus ($G = \tau/\gamma$) as strain amplitude increases. Ideally, the elastic soil's dynamic characteristic is not affected by variation in strain amplitude.

The shear modulus is considered unity for elastic materials, while the damping ratio is null [5]. Under cyclic loading, the nonlinearity of soil is influenced by the discreteness and the characteristic of elastic, perfectly plastic soil behavior. Increased soil discreteness reduces shear modulus, whereas less discrete soil exhibits a higher shear modulus. Conversely, the damping ratio behaves inversely to the shear modulus. Another critical factor that affects the nonlinear dynamic characteristic of the soil is the effective vertical stress in the soil, as illustrated in Fig. 1 (c), (e), and (f). In the soil column, two layers of sand at Layer 1 and 91 show different dynamic characteristics due to variations in effective stress. Higher effective stress increases the shear modulus and decreases the damping ratio for all soil layers. It shows that the effectiveness of dynamic properties diminishes under highly effective vertical stress, particularly in the sand at Layers 1 and 91, as shown in Fig. 1 (c). Similarly, the dynamic property of clay at Layer 13 is shown in Fig. 1 (e), and Fig. 1 (f) represents the gravel at Layers 85 and 96, illustrating the nonlinear dynamic properties under different effective stresses.

A one-dimensional nonlinear site response analysis is conducted in the nonlinear program DEEPSOIL [13] to anticipate the ground response, with scaled ground motions applied at the bedrock and propagated through nonlinear soil layers using the transfer function. Among the various soil modeling techniques, the General Quadratic/Hyperbolic Model (GQ/H) proposed by Groholski et al. [26] was used to model the soil layers. This model is suitable for simulating the backbone curve of soils, demonstrating strain hardening behavior at both small and large strains. A hyperbolic relation was generated to fit the shear modulus reduction curves from reference studies using the curve fitting parameters [13, 26]. The maximum shear strength (τ_{max}) was determined using Eq. (1) and directly incorporated into the program to construct the shear stress-strain curve. Additionally, a reduction factor introduced by Phillips and Hashash [27] was implemented to modify the unloading reloading behavior for the shear modulus reduction and damping curve fitting. Furthermore, the small strain frequency independent damping formulation was applied to eliminate the Rayleigh damping coefficients in DEEPSOIL.

This study performs the 1D nonlinear ground response analysis incorporating the specified soil column. Assuming the horizontal deviation of the soil layer is parallel and infinite. Reference backbone curves for sand and clay were adopted from Darendeli [28], while those for granular material were based on Menq [29]. The parametric soil data, including over-consolidation ratio (OCR), N value, and frequency (f), were set as 1, 10, and 1, respectively [28]. The plasticity index (PI) for clay was taken as 22% [30]. Due to the absence of experimental data, the dynamic properties of gravel were sourced from Menq [29], with a uniformity coefficient (Cu) of 20 and a median grain size (D50) of 8.0 mm. Using time-domain analysis, the soil column of depth 269 m was divided into 119 layers, ensuring a minimum frequency of 30 Hz. Additionally, elastic half-space properties were assumed for bedrock, with a shear velocity of 3200 Km/s, unit density of 24 KN/m^3, and damping ratio of 0.5% as rock outcrop motion was used for 1D site response analysis [31].

4 Result and discussion

4.1 PGA and acceleration time series variation with frictional angle

Peak ground acceleration (PGA) represents the maximum predicted ground acceleration from site response analysis using multiple strong ground motions. It anticipates the structure's seismic demand to resist the seismic energy encountered during an earthquake. In 1D ground response analysis, a deep soil column significantly influences the PGA at the surface. Each soil layer impacts the shear strength of the adjacent layers, which is governed by the soil's frictional angle. The variation of PGA due to changes in the frictional angle across soil layers in deep soil columns, as influenced by different ground motions, is collectively presented in a three-dimensional (3D) plot, as shown in Fig. 2. The result indicates that the maximum PGA of 0.249 g is observed at a 50-degree frictional

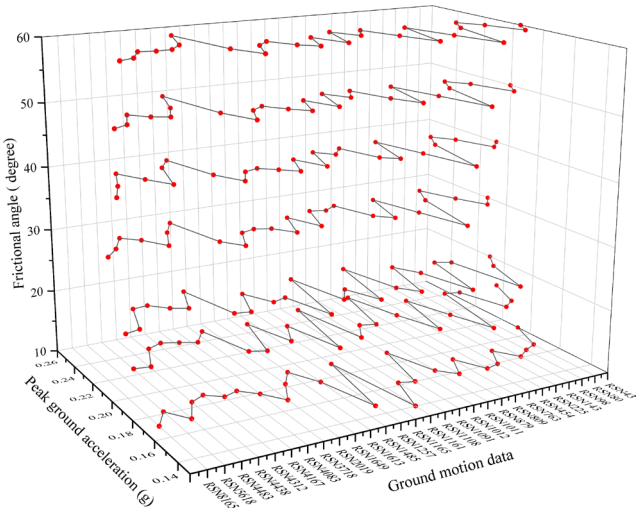

Fig. 2 A 3D visualization of the obtained PGA from the individual ground motion due to the influences of frictional angle during 1D site response analysis

angle, while a minimum PGA of 0.205 g is obtained at 10 degrees. Consistent PGA patterns remain across various ground motions, while soil frictional angles from 30 to 60 degrees are varied in site response analysis.

Meanwhile, the frictional angle below 30 degrees shows significant fluctuation in the PGA pattern depending on the ground motions. It is attributed to the soil layers' reduced shear strength, leading to weaker interlayer bonding. As the frictional angle increases beyond 30 degree, the shear strength and soil binding improve, resulting in more uniform PGA patterns across different ground motions, as depicted in Fig. 2.

A representative ground motion of two events, RSN 1108 (Kobe earthquake) and RSN 1485 (Chi-Chi earthquake), including PGA, are shown in Fig. 3. It encompasses the surface-level acceleration resulting from varying frictional angles. The acceleration time series motions demonstrate uniform behavior for frictional angles greater than 30 degrees, whereas notable distortion is observed for less than 30 degrees. In both cases, the maximum PGA was obtained at a frictional angle of 30 degree, with values of 0.233 g and 0.218 g, and minimum PGA values, 0.162 g and 0.178 g, were observed at a frictional angle of 10 degree for the Kobe and Chi-Chi earthquakes. This PGA and acceleration time series trend indicates greater uniformity at higher frictional angles. In contrast, deamplifiaction and a rightward shift in the PGA were observed from 30 to 60 degrees. However, below 30 degrees, the acceleration time series gradually decelerates, reaching minimum PGA at 10 degrees, as shown in Fig. 3. At this point, the PGA shifted further to the right and showed minimum PGA at 10 degree, deviating from the acceleration time series behavior than higher angles. Therefore, during one-dimensional site response analysis, a 30-degree frictional angle yields maximum PGA and higher acceleration time series than other frictional angles.

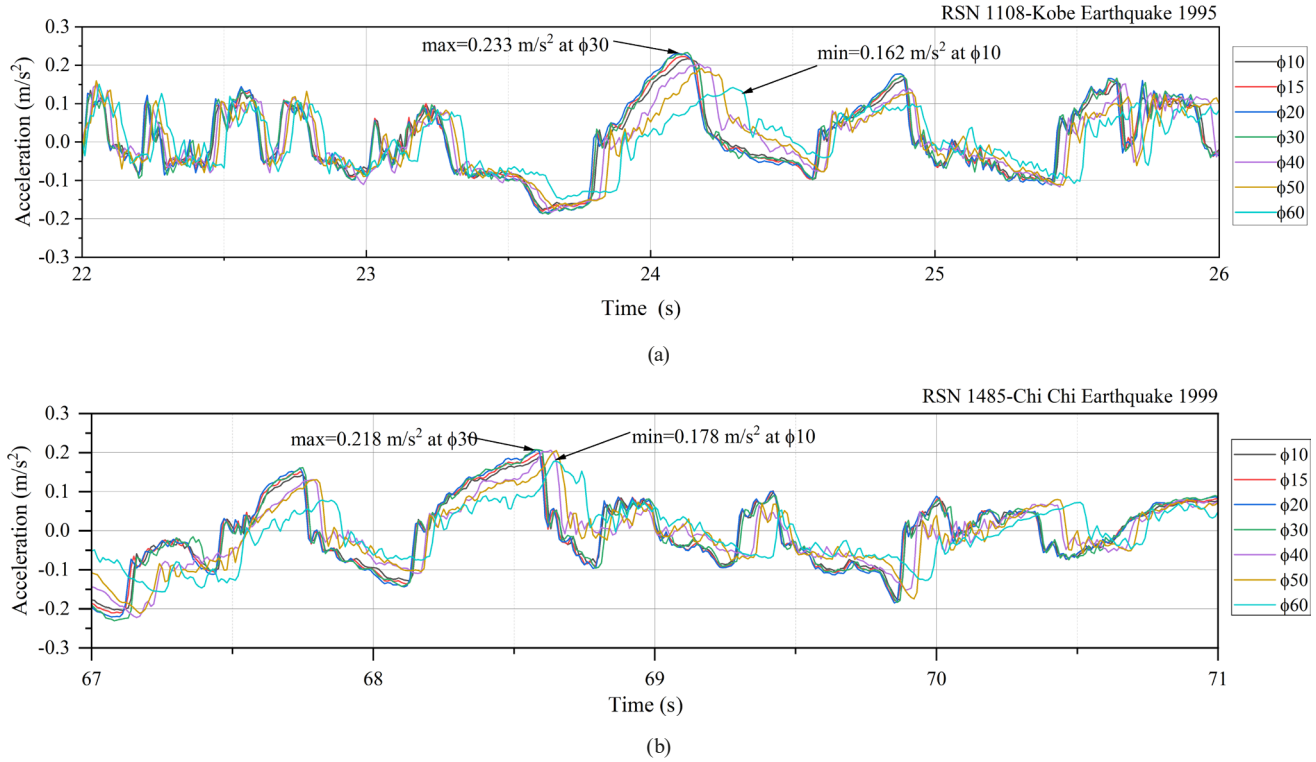

Fig. 3 Time history obtained from the 1D site response analysis due to change in frictional angle representing the maximum and minimum PGA (a) time history of Kobe earthquake 1995 (RSN1108) (b) time history of Chi Chi earthquake 1999 (RSN1485)

At the top layer, the soil's dynamic behavior is governed predominantly by the shear strength interaction with the adjacent lower soil layer. Fig. 1 shows the shear modulus and damping ratio of all the frictional angles in the same plot, which crosses at a point while increasing in strain value. It exhibits high dynamic property values at low shear strain, particularly for a frictional angle of 60 degree. As shear strain increases, the coincide point of the frictional angles decreases, reaching a minimum at 30 degree. Beyond 30 degrees, the coinciding point's dynamic properties rise with increased shear strain. This phenomenon explains why the obtained PGA for the 30-degree frictional angle has maximum value as the dynamic properties decrease at the critical section.

4.2 Influences of PGA due to frictional angle, magnitude, and distance of earthquakes

Fig. 4 illustrates the influences of the soil frictional angle on the prediction of PGA. The results demonstrate a range of PGAs for each examined frictional angle, with the minimum values occurring at 10 degrees and the maximum observed at 50 degree. At a frictional angle of 10 degree, the soil exhibits low shear strength, leading to loose energy dissipating behavior that causes over-softening, thereby reducing PGA. Conversely, high stress is required for very dense soil to generate shear strain between soil layers due to damping effects. The maximum PGA response is obtained for dense soil with soil's frictional angle 30 to 50-degree.

Further, for all examined ground motions, the maximum and minimum PGA is well fitted into the second-order polynomial equation with R^2 values 0.97 and 087, as presented in Eqs. (2) and (3). The average PGA range, on the other hand, is best fitted with third-degree polynomial Eq. (4) with a R^2 value of 0.99, as shown in Fig. 4 (b).

$$y = (0.17707 \pm 0.005) + (0.0035 \pm 3.44573 \times 10^{-4}) * x + (-4.12049 \times 10^{-5} \pm 4.88119 \times 10^{-6}) * x^2 \quad R^2 = 0.97 \tag{2}$$

$$y = (0.11544 \pm 0.01002) + (0.00353 \pm 6.90566 \times 10^{-4}) * x + (-4.68954 \times 10^{-5} \pm 9.7825 \times 10^{-6}) * x^2 \quad R^2 = 0.87. \tag{3}$$

$$y = (0.10814 \pm 0.00534) + (0.0035 \pm 3.44573 \times 10^{-4}) * x + (-4.12049 \times 10^{-5} \pm 4.88119 \times 10^{-6}) * x^2 + (1.31936 \times 10^{-6} \pm 1.78246 \times 10^{-7}) * x^3 \quad R^2 = 0.99 \tag{4}$$

Fig. 5 (a) and (b) compare the predicted PGA with earthquake magnitude and rupture distance, respectively. The prediction is based on data from 28 earthquakes ranging from 4.9 to 7.4 Mw and distances from 0 to 60 m. The influence of earthquake magnitude and rupture distance on PGA prediction appears to have minimal effects, showing a similar range of PGA values across the dataset. However, for 6.0 Mw and 6.3 Mw magnitudes, the predicted PGA fluctuates from maximum to minimum,

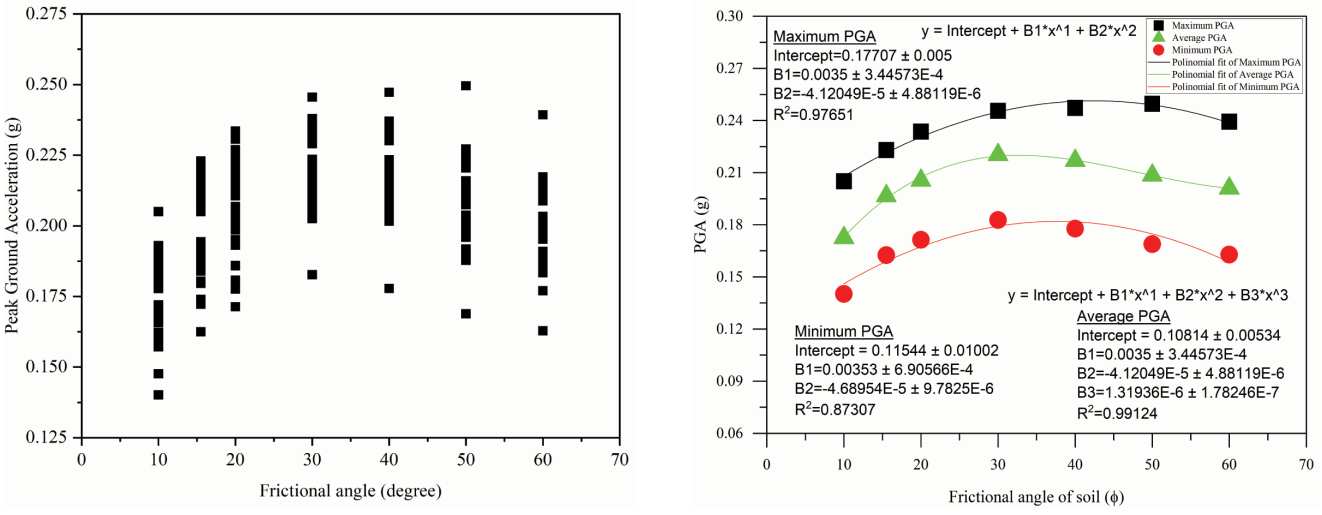

(a) (b)

Fig. 4 (a) Obtained PGA according to the change in frictional angle (b) Polynomial curve fit of maximum, minimum, and average PGA to anticipate the PGA with a frictional angle of soil

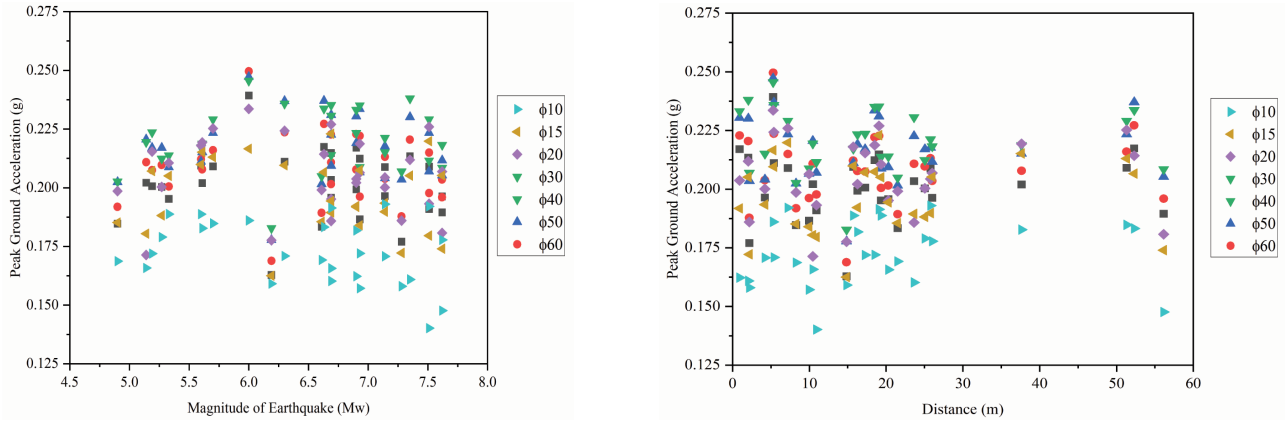

Fig. 5 (a) Comparision of obtained PGA with the magnitude of earthquake (b) Comparision of PGA with the epicentre distance

while other earthquake magnitudes show consistent PGA ranges. For a frictional angle of 10 degrees, lower PGA values are predicted with higher earthquake magnitude, whereas other degrees of frictional angle have a random prediction. Likewise, PGA predictions exhibits random variation with both near and far epicentral distances, similar to that of earthquake magnitude.

The nonlinear dynamic properties of soil layers play a critical role in transmitting seismic ground motions from bedrock to the surface. The amplification or deamplification of PGA is influenced by the nonlinear behavior of the soil, which dissipates energy as a seismic wave passes through it. The one-dimensional site response analysis on the deep sediment column reveals the deamplification of PGA, as shown in Fig. 6, which compares the ratio of PGA from surface to bedrock. The highest deamplification occurs at 10-degree frictional angle, with an average ratio of 0.47. Similarly, the least reduction in PGA is 0.59, observed at 30 degrees. Overall, the average PGA reduction during site response analysis is 0.55.

4.3 Effects of frictional angle in strain depth

The soil deformation during an earthquake is influenced by the amount of shear strain experienced within soil layers. The nonlinear dynamic properties of soil, comprising the damping ratio and shear modulus, are anticipated to alter according to the change in the soil's frictional angle. Relative variations in shear strain with depth are generally associated with soil layer deformation during ground motion. Fig. 7 depicts the variation of shear strain with depth as a function of soil frictional angle, highlighting the maximum average shear strain of the soil models occurring at 11.5 m depth from the surface. During site response analysis, two distinct peaks in the shear strain plot were obtained at 6.5 m and 11.5 m for frictional angles 10 and 30 degree, such that the maximum average shear strain

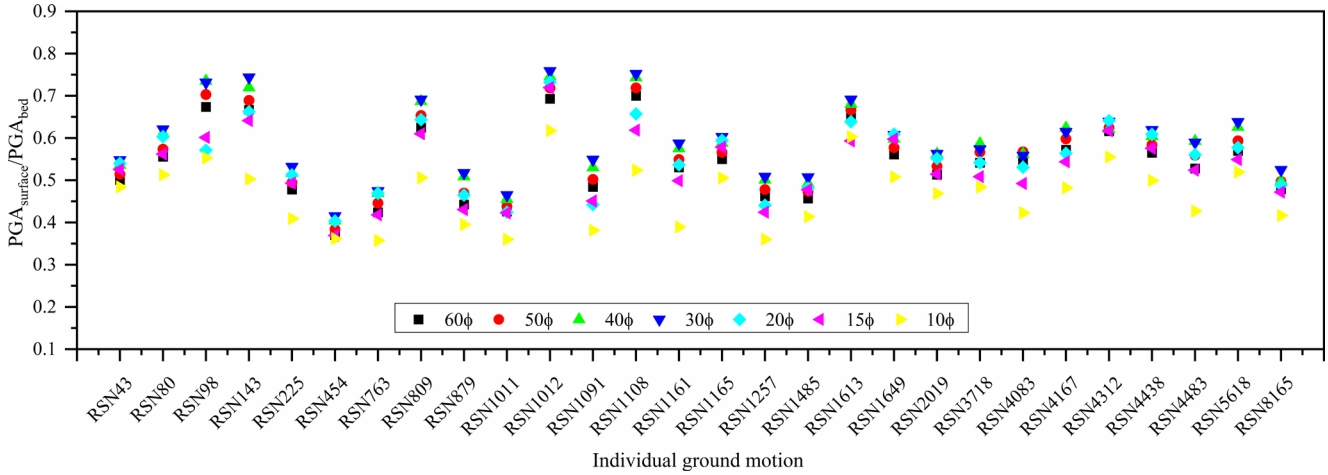

Fig. 6 Amplification of obtained PGA of an individual earthquake for PGA of earthquake applied to bedrock

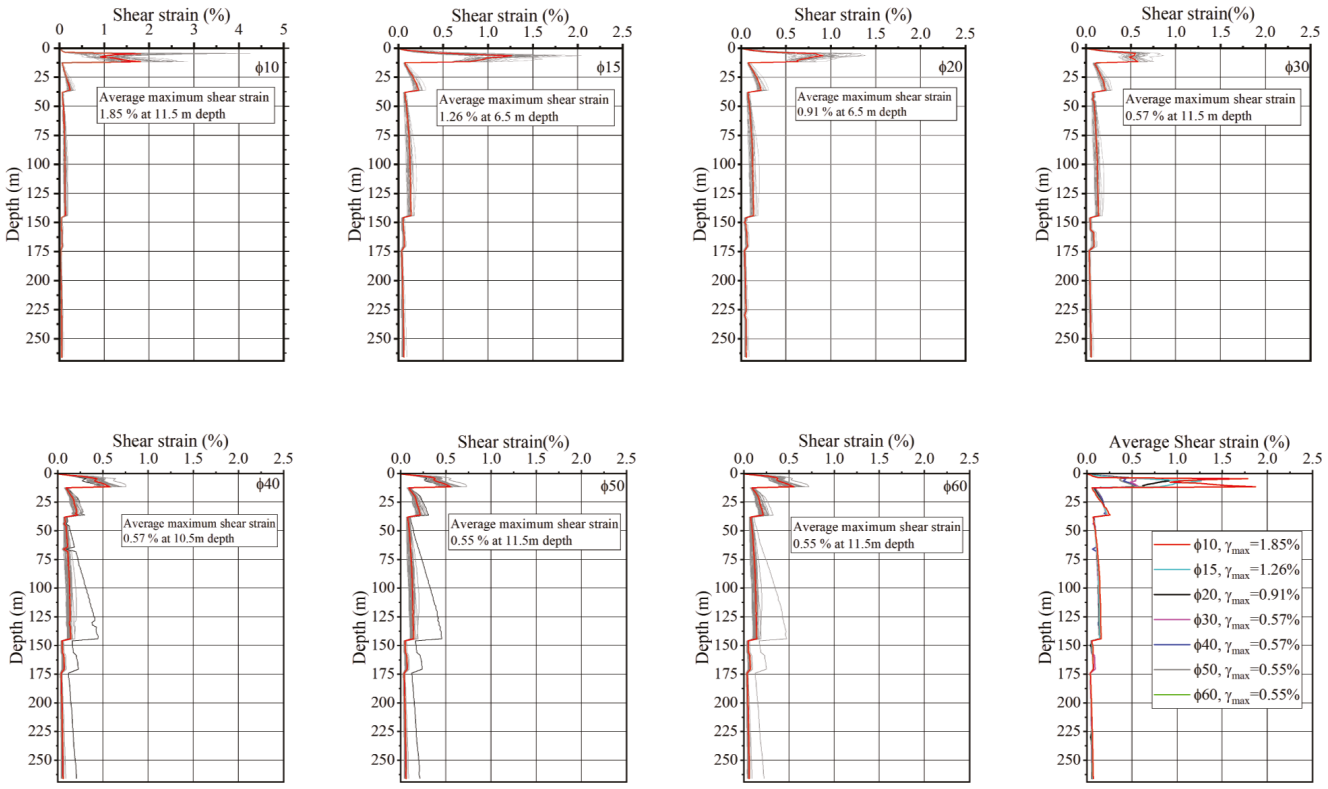

Fig. 7 Individual shear strain to depth due to the application of frictional angle of soil from 0 to 60 degree and its comparison

was 1.85% and 0.57% at 11.5 m, respectively. However, frictional anlges of 15 and 20 degree exhibit single peaks of maximum shear strain at 6.5 m, with values 1.26% and 0.91%, respectively. All other frictional angles displayed a maximum shear strain of 0.55% at 11.5 m from the surface. Beyond a depth of 16m, the shear strain shows no significant changes while varying friction, as shown in Fig. 7. The maximum shear strain of 1.867% was recorded for a 10 degree friction angle, likely due to the reduced shear resistance in lower soil friction. Likewise, the presence of sand layers at the shallow depth contributes to higher deformation of soil layers during ground shaking, leading to higher shear strains near the surface.

The combination of sand layers in the upper soil and lower effective stress at the near-surface causes considerable undulations in shear strain up to a depth of 16 m. In all cases, the soil masses experience excessive softening and damping, as the peak shear strain at shallow depth is significantly higher than the residual shear strain with depth. Fig. 7 (h) compares the effect of varying frictional angles on shear strain with depth. It shows that, regardless of changes in frictional angle, there is no substantial variation in shear strain at deeper depths. Table 2 demonstrates that shear strength to effective vertical stress ratios remain relatively stable for frictional angles greater than 30 degree, accounting for the lack of significant changes in peak shear strain at higher angles. In contrast, a significant alternation in peak shear strain was observed below 30 degrees frictional angle, corresponding to notable changes in the shear strength to stress relationship. As a result, at shallow depths, loose soil with a low frictional angle experiences significant soil deformation, resulting in a pronounced divergence in shear stress to strain behavior.

4.4 Influences of frictional angles in response spectra

The determination of appropriate spectral acceleration in deep sediment deposits requires analyzing soil layers with varying frictional angles. Fig. 8 illustrates the influence of soil's frictional properties on spectral acceleration across several soil layers of sand, clay, and gravel from the deep deposit. In the soil column model, sand is represented by layers 1 and 91, gravel by layers 85 and 96, and clay by layer 13. The selection of spectral acceleration at different depths is based on significant changes in the impedance ratio between adjacent layers, Layers 1, 13, and 85, demonstrating similar spectral acceleration trends, regardless of frictional angle, showing short-period wave dominance. Meanwhile, layers 91 and 96 exhibit more variation in spectral behavior, reflecting the influence of long-period waves. The transition between soil layers,

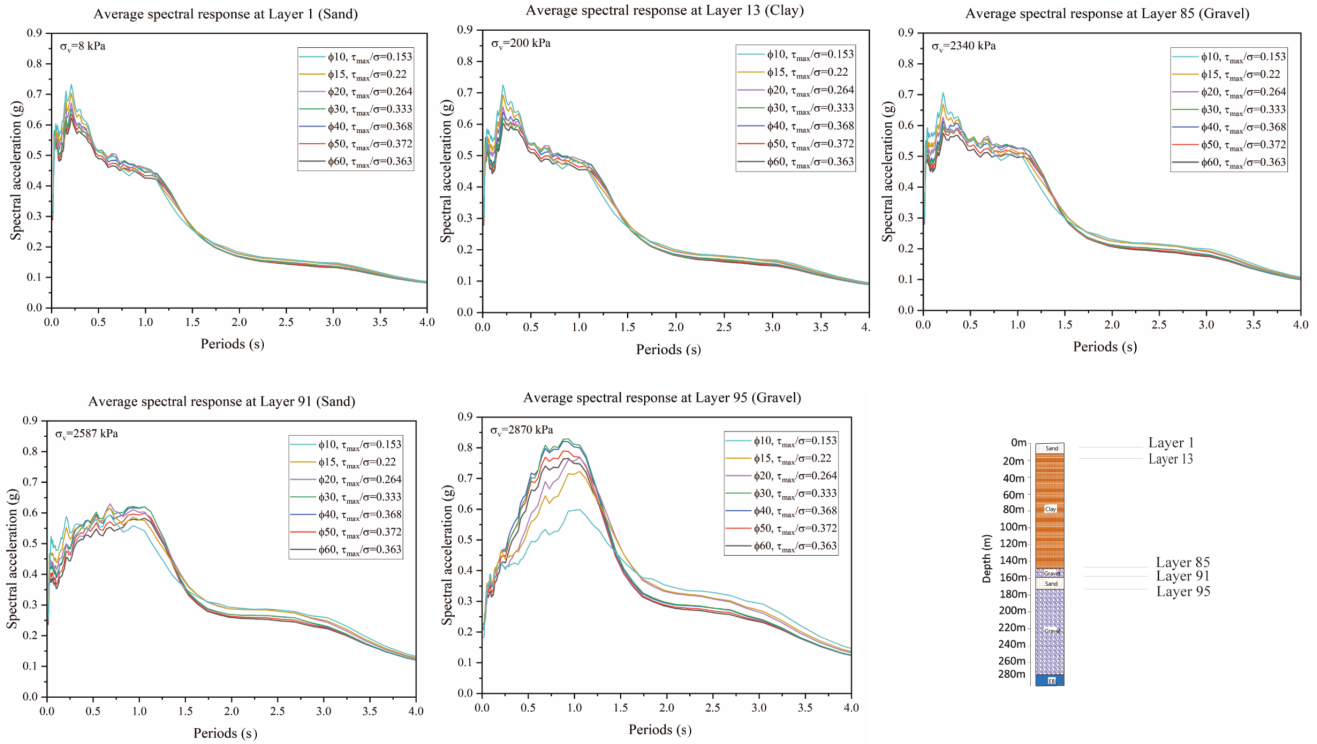

Fig. 8 Spectral acceleration generated from 0 to 60 degree frictional angle of soil at different layers of soil column

from gravelly sand to clay, significantly impacts the seismic response. It is mainly observed in the sand at depths corresponding to Layers 1 and 96. However, Layer 1 is similar to the response of the clay layer due to the comparatively lower impedance ratio between them. Referring to Fig. 1, the friction angle does not drastically alter the overall response in different types and layers of soil, contributing to a similar seismic response. At higher stresses, the soil behavior is nonlinear. The nonlinearity does not lead to drastic differences in spectral response across the layer due to the damping effects at higher strains, which tend to moderate the response. Thus, the upper three layers produce similar spectral shapes across different layers.

In short-period dominant response spectra, the maximum response across all layers is observed for a frictional angle 10 degree, while the minimum is 60 degrees. At long-period dominant spectra, the maximum spectral acceleration is generated when the frictional angle is 30 degree. It shows that shear modulus reduction becomes insignificant, particularly in sand layers 91 and gravel layers 85 and 96, due to a substantial increase in effective stress. Lower effective vertical stress produces a higher spectral response of around 0.2 seconds, whereas higher stress yields a greater response of around 1.05 seconds. The varying responses in the sand and gravel layers are influenced by the effective stress acting on each layer.

The spectral response curve displays a broad peak from 0.22 seconds to 1.05 seconds, with all layers exhibiting higher spectral acceleration up to 1.05 seconds. Following this, the curve sharply declines at 1.75 seconds, with a gradual decrease observed afterward. At longer period the differences in spectral acceleration between all layers become less pronounced for all frictional angles. In the upper layers, a notable spectral acceleration spike occurs around 0.2 seconds for the top three layers. Interestingly, in the deeper layers, spectral acceleration increases at longer period, forming a concave downward curve, while in the short period range, the spike diminishes with rising effective stress. This pattern suggests that effective stress influences the peak spectral acceleration, causing it to decrease at short period and increase at longer period.

4.5 Seismic response in various depths due to frictional angle

The response of deep sediment layers in the 1D site analysis to varying frictional angles, ranging from 10 to 60 degree, is depicted in Fig. 9. The analysis reveals that the top three layers experience peak spectral acceleration over short period, while the bottom two layers show peak response during long period across all frictional angle. The higher spectral response for the 10 degree frictional angle at short period is attributed to the low shear strength

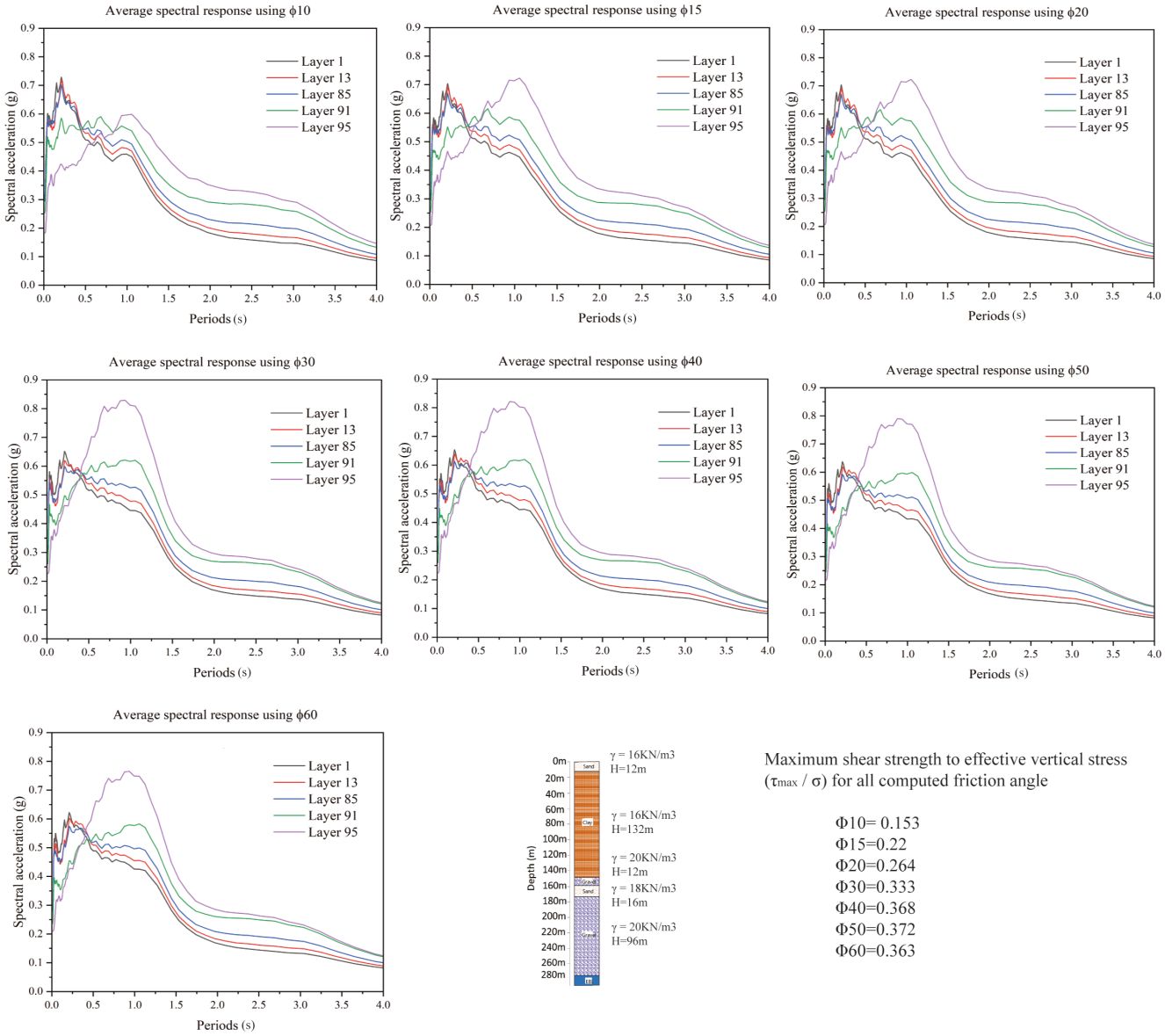

Fig. 9 Spectral acceleration plots at a different layer of deep soil colum from 0 to 60 degree frictional angle of soil

and low effective stress at the uppermost layer. Due to the changes in effective stress that affect the nonlinear properties of the soil, as outlined in Section 4.4, the sand and gravel layers exhibit different responses at various strata. A higher frictional angle leads to higher spectral responses in the lower layers at longer periods, whereas a lower frictional angle results in elevated spectral responses in the upper layers during shorter periods, as shown in Fig. 9.

In general, frictional angle and effective stress contribute to an increase in shear strength. As shown in Table 2, the ratio of shear strength to vertical effective stress differs for each frictional angle. This ratio increases as the frictional angle rises, with the lowest ratio observed at 10 degree and the highest at 50 degree. Notably, the maximum ratio is observed at 50 degrees, attributed to the rapid increase in shear strength surpassing the rise in effective stress. These frictional characteristics are key factors in predicting the maximum peak ground acceleration during seismic motion and the behavior of the acceleration time series.

5 Conclusions

The nonlinear seismic response of deep sediment soil to seismic events is examined using a one-dimensional ground response software, DEEPSOIL, with available soil data. The study explored a range of soil friction angles from 10 to 60 degrees, to account for variations in the soil's dynamic properties. The transfer function uses around 28 bed outcrop ground motions to transmit horizontal motions to each soil layer. An examination of deep sediment columns with multiple soil layers was conducted

at different depths where the impedance ratio fluctuated. It was noted that when the effective vertical stress increases with depth, a notable change is observed in the dynamic properties of the soil. This study computed how the variations in soil friction angle affected the site PGA, strain amplitude, and spectra response. The results provide insights into the impact of different frictional angles on the nonlinear seismic behavior of deep sedimentary deposits and their implications for site-specific hazard assessments:

1. Variation in the soil frictional angle influences the soil's discreteness, revealing a high PGA value at 30 degrees and a low PGA at 10 degrees. The result demonstrates dense soil with frictional angles between 30 and 50 degrees has a higher PGA than very loose soil.
2. The PGA amplification from bedrock to surface ranges from 0.47 to 0.59, and the average PGA reduction across all friction angles is 0.55. The average PGA with respect to the friction angle plot is best fitted for the third-degree polynomial relation, with the R^2 value of 0.99. Similarly, the maximum and minimum PGA from the varying frictional angle fit a second-degree polynomial curve, with R^2 values 0.97 and 0.87, respectively.
3. The nonlinear 1D site response analysis shows that a change in the soil's frictional angle from 30 to 60 degrees generates no significant strain, with a maximum strain of 0.57% at 11.5 meters. However, the highly discrete soil that acquires less frictional angle generates a higher strain of 1.85% at 11.5 meters.
4. No significant difference in the spectral response was observed at long-period response spectra due to a change in the soil's discreteness by the increase of effective vertical stress. However, a 10-degree frictional angle at a short period (0.2 s) at the top layer and a 30-degree frictional angle for the deeper layer having high vertical stress at long periods (1.05 s) resulted in a higher spectral response.

Acknowledgment

The authors appreciate the detailed review of the anonymous reviewers, whose suggestions greatly improved this article.

Declaration of conflicting interests

The author(s) declared no potential conflicts of interest concerning this article's research, authorship, and/or publication.

Funding

This work was financially supported by the State Key Laboratory of Disaster Reduction in Civil Engineering (Grant No. SLDRCE19-B-29).

References

[1] Whittaker, A., Atkinson, G., Baker, J., Bray, J., Grant, D., Hamburger, R., Haselton, C., Somerville, P. "Selecting and Scaling Earthquake Ground Motions for Performing Response History Analyses", Engineering Laboratiory of the National Institute of Standards and Technology, National Institute of Standards and Technology (NIST), Gaithersburg, MD, USA, Rep. NISTGCR 11-917-15, 2011.

[2] CEN "CEN EN 1998-1:2004 Eurocode 8: Design of structures for earthquake resistance - Part 1: General rules, seismic actions and rules for buildings", European Committee for Standardization, Brussels, Belgium, 2004.

[3] Lamichhane, S., Luke, B. "Input ground motions for earthquake site response analyses: deep sediment column with cementation", International Journal of Geotechnical Engineering, 10(2), pp. 190–204, 2016. https://doi.org/10.1080/19386362.2015.1113354

[4] Zahoor, F., Satyam, N., Rao, K. S. "A Comprehensive Review of the Nonlinear Response of Soil Deposits and its Implications in Ground Response Analysis", Indian Geotechnical Journal, 54(3), pp. 781–799, 2024. https://doi.org/10.1007/s40098-023-00798-1

[5] Towhata, I. "Geotechnical Earthquake Engineering", Springer, 2008. ISBN 978-3-540-35782-7 https://doi.org/10.1007/978-3-540-35783-4

[6] Kokusho, T. "In-situ dynamic soil properties and their evaluations", In: 8th Asian Regional Conference on Soil Mechanics and Foundation Engineering, 1987, vol. 2, pp. 215–240. ISBN 4-88644-802-X

[7] Kramer, S. L. "Geotechnical Earthquake Engineering", Prentice Hall, 1996. ISBN 9780133749434

[8] Idriss, I. M., Seed, H. B. "An analysis of ground motions during the 1957 San Francisco earthquake", Bulletin of the Seismological Society of America, 58(6), pp. 2013–2032, 1968. https://doi.org/10.1785/bssa0580062013

[9] Kaklamanos, J., Baise, L. G., Thompson, E. M., Dorfmann, L. "Comparison of 1D linear, equivalent-linear, and nonlinear site response models at six KiK-net validation sites", Soil Dynamics and Earthquake Engineering, 69, pp. 207–219, 2015. https://doi.org/10.1016/j.soildyn.2014.10.016

[10] Aimar, M., Foti, S. "Simplified Criteria to Select Ground Response Analysis Methods for Seismic Building Design: Equivalent Linear versus Nonlinear Approaches", Bulletin of the Seismological Society of America, 111(4), pp. 1940–1953, 2021. https://doi.org/10.1785/0120200319

[11] Kim, B., Hashash, Y. M. A., Stewart, J. P., Rathje, E. M., Harmon, J. A., Musgrove, M. I., Campbell, K. W., Silva, W. J. "Relative Differences between Nonlinear and Equivalent-Linear 1-D Site Response Analyses", Earthquake Spectra, 32(3), pp. 1845–1865, 2016. https://doi.org/10.1193/051215EQS068M

[12] Conti, R., Angelini, M., Licata, V. "Nonlinearity and strength in 1D site response analyses: a simple constitutive approach", Bulletin of Earthquake Engineering, 18(10), pp. 4629–4657, 2020. https://doi.org/10.1007/s10518-020-00873-5

[13] Hashash, Y. M. A., Musgrove, M. I., Harmon, J. A., Ilhan, O., Xing, G., Numanoglu, O., Groholski, D. R, Phillips, C. A., Park, D. "DEEPSOIL V7.0, User Manual", Board of Trustees of University of Illinois at Urbana-Champaign, Urbana, IL, USA, 2020.

[14] Bolisetti, C., Whittaker, A. S., Mason, H. B., Almufti, I., Willford, M. "Equivalent linear and nonlinear site response analysis for design and risk assessment of safety-related nuclear structures", Nuclear Engineering and Design, 275, pp. 107–121, 2014. https://doi.org/10.1016/j.nucengdes.2014.04.033

[15] Xiao, M., Cui, J., Li, Y., Nguyen, V.-Q. "Nonlinear Seismic Response Based on Different Site Types: Soft Soil and Rock Strata", Advances in Civil Engineering, 2022, 5370369, 2022. https://doi.org/10.1155/2022/5370369

[16] Meite, R., Wotherspoon, L., Kaklamanos, J., McGann, C. R., Hayden, C. "Sensitivity of 1-D ground motion predictions to analysis codes and material models using KiK-net vertical arrays", Soil Dynamics and Earthquake Engineering, 133, 106113, 2020. https://doi.org/10.1016/j.soildyn.2020.106113

[17] Kim, H. "Comparison of Site Response Analysis (SRA) According to Ground Modelling and Structure Consideration", In: Salazar, W. (ed.) Earthquake Ground Motion, IntechOpen, 2023, Chapter 6. ISBN 978-0-85466-221-0 https://doi.org/10.5772/intechopen.1002922

[18] Bard, P.-Y., Gariel, J.-C. "The seismic response of two dimensional sedimentary deposits with large vertical velocity gradients", Bulletin of the Seismoligical Society of America, 76(2), pp. 343–366, 1986. https://doi.org/10.1785/BSSA0760020343

[19] Nguyen, V.-Q., Aaqib, M., Nguyen, D.-D., Luat, N.-V., Park, D. "A Site-Specific Response Analysis: A Case Study in Hanoi, Vietnam", Applied Sciences, 10(11), 3972, 2020. https://doi.org/10.3390/app10113972

[20] Poland, C., D., Mitchell, A. D. "A New Seismic Rehabilitation Standard - ASCE/SEI 41-06", In: New Horizons and Better Practices, Long Beach, CA, USA, 2012, 1–2. ISBN 9780784409466 https://doi.org/10.1061/40946(248)35

[21] Pacific Earthquake Engineering Research Center "PEER Ground Motion Database", [online] Available at: https://ngawest2.berkeley.edu/ [Accessed: 15 April 2023]

[22] Parajuli, H. R., Bhusal, B., Paudel, S. "Seismic zonation of Nepal using probabilistic seismic hazard analysis", Arabian Journal of Geosciences, 14(20), 2090, 2021. https://doi.org/10.1007/s12517-021-08475-4

[23] Al Atik, L., Abrahamson, N. "An Improveded Method For Nonstationary Spectral Matching", Earthquake Spectra, 26(3), pp. 601–617, 2010. https://doi.org/10.1193/1.3459159

[24] Kawan, C. K., Maskey, P. N., Motra, G. B. "A Study of Local Soil Effect on the Earthquake Ground Motion in Bhaktapur City, Nepal Using Equivalent Linear and Nonlinear Analysis", Iranian Journal of Science and Technology, Transactions of Civil Engineering, 46, pp. 4481–4498, 2022. https://doi.org/10.1007/s40996-022-00858-1

[25] Régnier, J., Bonilla, L.-F., Bard, P.-Y., Bertrand, E., Hollender, F., Kawase, H., …, Watanabe, K. "International Benchmark on Numerical Simulations for 1D, Nonlinear Site Response (PRENOLIN): Verification Phase Based on Canonical Cases", Bulletin of the Seismological Society of America, 106(5), pp. 2112–2135, 2016. https://doi.org/10.1785/0120150284

[26] Groholski, D. R., Hashash, Y. M. A., Kim, B., Musgrove, M., Harmon, J., Stewart, J. P. "Simplified Model for Small-Strain Nonlinearity and Strength in 1D Seismic Site Response Analysis", Journal of Geotechnical and Geoenvironmental Engineering, 142(9), 04016042, 2016. https://doi.org/10.1061/(asce)gt.1943-5606.0001496

[27] Phillips, C., Hashash, Y. M. A. "Damping formulation for nonlinear 1D site response analyses", Soil Dynamics and Earthquake Engineering, 29(7), pp. 1143–1158, 2009. https://doi.org/10.1016/j.soildyn.2009.01.004

[28] Darendeli, M. B. "Development of a new family of Normalized modulus reduction and material damping curves", Doctor of Philosophy Dessertation, The University of Texas Austin, 2001.

[29] Menq, F.-Y. "Dynamic Properties of Sandy and Gravelly Soils", Doctor of Philosophy Dissertation, The University of Texas Austin, 2003.

[30] Gilder, C. E., Pokhrel, R. M., Vardanega, P. J., De Luca, F., De Risi, R., Werner, M. J., Asimaki, D., Maskey, P. N., Sextos, A. "The SAFER geodatabase for the Kathmandu Valley: Geotechnical and geological variability", Earthquake Spectra, 36(3), pp. 1549–1569, 2020. https://doi.org/10.1177/8755293019899952

[31] Bijukchhen, S. M. "Construction of 3-D Velocity Structure Model of the Kathmandu Basin, Nepal Based on Geological Information and Earthquake Ground Motion Records", Doctor of Engineering Thesis, Hokkaido University, 2018. https://doi.org/10.14943/doctoral.k13350